26 Exoplanet Atmospheres

26.1 *Temperatures*

Like stars or brown dwarfs, planets are born hot. But they cool off quickly, and so the energy budgets of all but the youngest exoplanets are dominated by stellar irradiation reprocessed by the planet's atmosphere (or surface). When internal heat sources are small, a planet in energy balance should satisfy

$$E_{\rm out} = E_{\rm abs} = (1 - A_B) E_{\rm inc} \tag{774}$$

where the E's above are the outgoing (emitted), absorbed, and incident energies, respectively. The term A_B is the **Bond Albedo** of a planet, and indicates the bolometric fraction of incident energy absorbed by the planet. (Thus the reflected energy is $A_B E_{\rm inc}$ — shinier planets reflect, i.e. scatter, more light.)

Given a planet with radius R_p, orbital separation a, and stellar radius R_*, energy balance then implies that over the entire planet

$$4\pi R_p^2 F_p = (1 - A_B) \left(\frac{R_*}{a} \right)^2 \pi R_p^2. \tag{775}$$

Invoking the Stefan-Boltzmann law for the star in terms of its effective temperature $T_{\rm eff}$, we can then calculate the **equilibrium temperature** of the planet's irradiated day side,

$$T_{\rm eq} = T_{\rm eff} \left(\frac{R_*}{a} \right)^{1/2} \left[f \left(1 - A_B \right) \right]^{1/4} \tag{776}$$

Here f accounts for the fact that on a planet with an atmosphere (or ocean), bulk motion can transport heat from the hot day side to the colder night side: in this case the planet effectively radiates with a greater effective surface area, and so $T_{\rm eq}$ is lower. Valid values of f range from $1/4$ (lower $T_{\rm eq}$, indicating full heat circulation around the planet) to $2/3$ (no circulation). Note that the equilibrium temperature is really just a parameterized incident irradiation that lets us sweep our uncertainty about f and A_B under the rug. There is also an **irradiation temperature**,

$$T_{\rm irr} = T_{\rm eff} \left(\frac{R_*}{a} \right)^{1/2} = \frac{S_0^{1/4}}{\sigma_{SB}} \tag{777}$$

which describes the incident radiation coming in at the substellar point (noon on the equator). Here S_0 is (for Earth) the **Solar constant** of about 1400 W m^{-2} incident at the top of the atmosphere.

Typical values for A_B are 0.12 for Mercury, 0.75 for Venus, and $\sim$0.3 for the other Solar system planets. Thus Venus actually has a lower $T_{\rm eq}$ than the Earth despite being closer to the Sun (i.e., having greater $T_{\rm irr}$). Nonetheless the Venerean surface is hot enough to melt lead. This hints at a key issue with the use of equilibrium temperature: it is only a rough proxy and can sometimes lead to expectations at variance with observations.

We know comparatively little about the albedos of most exoplanets. Most measurements to date are of hot Jupiters (highly irradiated gas giants, $T_{\rm eq} > 1000$ K and $R_p \sim R_{\rm Jup}$) and indicate quite low albedos, $A_B \lesssim 0.2$. But a few exceptions have quite high albedos; these are thought to be covered in especially reflective clouds.

26.2 *Surface-Atmosphere Energy Balance*

It may surprise you to consider that some planets have atmospheres, which can absorb and emit radiation on their own. If the planet also has a solid surface, then we can equate the radiation absorbed and re-emitted by both the atmosphere and the surface to gain insight into the planet's energy balance.

The overall picture is shown in Fig. 63. The scenario is similar in some ways to the two-layer stellar model introduced in Sec. 7.2, but now we have a surface. We split the radiation into two wholly separate components: incoming radiation from the star, and outgoing radiation from the surface and atmosphere. For the Earth around the Sun, $T_P \approx 290$ K and $T_* \approx 5800$ K, so from Wien's Law (Eq. 82) $\lambda_{P,\rm max} \approx 10\mu$m while $\lambda_{*,\rm max} \approx 500$ nm. These very different wavelengths are not typically affected by the same opacity sources, and so we are justified in treating these two radiation streams separately. For hotter planets and/or cooler stars, this assumption can break down: e.g. the hottest of the hot Jupiters have $T_{\rm eq} \gtrsim 2000$ K, not so much cooler than the coolest stars.

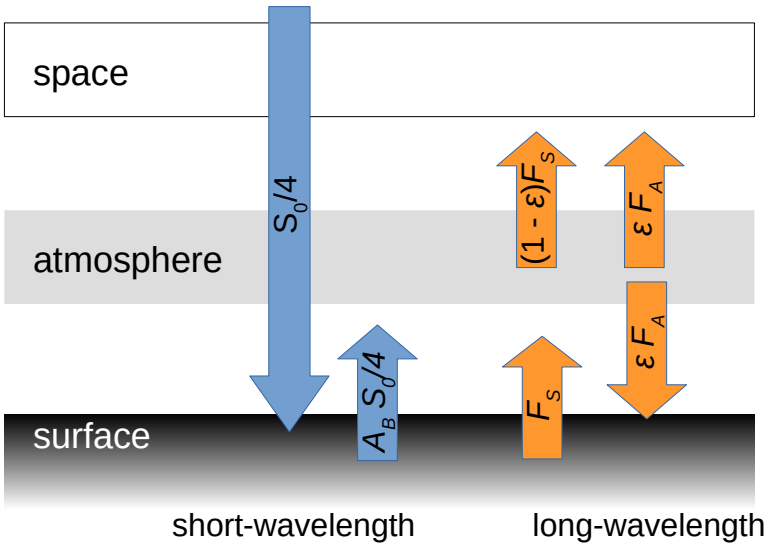

Figure 63: Energy balance on a planet with an atmosphere. Short-wavelength (visible) radiation is shown in blue, and long-wavelength (thermal) radiation in orange.

We assume that the atmosphere has a thermal emissivity ϵ, where

$$\epsilon = 1 - e^{-\tau}. \tag{778}$$

For a fairly thin atmosphere (like the Earth's), $\tau < 1$ and so $\epsilon \approx \tau$. We will define F_S and F_A as the flux emitted by a blackbody at the temperatures of the surface and atmosphere, respectively.

If we require energy balance at the planet's surface, we have

$$\frac{S_0}{4} + \epsilon F_A = \frac{A_B S_0}{4} + F_S. \tag{779}$$

The atmosphere is transparent to the incoming radiation but absorbs some of the thermal radiation from the surface, so atmospheric energy balance gives

$$\epsilon F_S = 2\epsilon F_A. \tag{780}$$

Combining these two relations gives

$$\sigma T_S^4 = S_0 \frac{1 - A_B}{4} \frac{1}{1 - \epsilon/2} \tag{781}$$

which relates the surface temperature T_S to the planetary albedo and atmospheric emissivity. If A_B is low the planet's surface will cool off – but as the atmosphere becomes more opaque to thermal radiation (i.e., as ϵ rises from $\sim$0 toward unity) the surface temperature will increase. This second point is one simple version of the **greenhouse effect**. It is part of the reason that Venus' surface is much hotter than its upper atmosphere (i.e., because $\epsilon_{\text{Venus}} \approx 1$), and is one reason that Earth's surface temperature is slowly but steadily increasing (i.e., because $\epsilon_\oplus$ is being increased).

If one sets T_S to 273 K and 373 K, with reasonable values of ϵ one can calculate the inner and outer orbital semimajor axes a for which liquid water can persist on the planet's surface. This is the first step toward calculating the **habitable zone**; planets in this zone orbiting a star are often particularly intriguing prospects for atmospheric characterization.

26.3 *Transmission Spectroscopy*

Long ago in Sec. 4.3 we briefly alluded to transiting planets. The transit method is the most productive method to date for finding new planets; it also provides a way to study the chemical composition of their atmospheres. This is useful because planets are so much fainter than stars that measuring their composition via spectroscopy of their thermal emission (as we do with stars) is impossible in all but a few of the most favorable cases. Instead, we use **transmission spectroscopy**.

In an atmosphere in hydrostatic equilibrium (Eq. 192), the pressure is

$$P = nkT = P_0 e^{-z/H} \tag{782}$$

where H is the **atmospheric scale height**, the characteristic e-folding scale of

the atmosphere:

$$H \equiv \frac{k_B T}{\mu g_P}. \tag{783}$$

If we assume that the atmosphere is isothermal, then similarly

$$n(z) = n_0 e^{-z/H}. \tag{784}$$

When observing a transit at a particular wavelength, we will only observe down to an altitude z such that the tangent optical depth is roughly unity. The ray will travel from one side of the atmosphere through to the other, with a minimum altitude z. The full optical depth along that tangent line is

$$\begin{aligned}\tau_\nu &= 2\int_z^R n\sigma_\nu ds \\ &= 2\sigma_\nu n_0 \int_z^R e^{-r/H} ds.\end{aligned}$$

Due to the dependence of z and s this integral isn't totally trivial. What's important is that n drops off rapidly (exponentially!) with altitude, so that the optical depth is dominated by the minimum altitude z hit by the ray. This means that

$$\tau_\nu \propto e^{-z/H} = 1. \tag{785}$$

Because z depends on the opacity — which is wavelength-dependent — a different altitude is reached for the rays at each wavelength. If we observe transits at two different wavelengths, then the two altitudes probed will be

$$\frac{z_1 - z_2}{H} = \frac{\delta z}{H} = \ln \frac{\sigma_1}{\sigma_2}. \tag{786}$$

The result is that each transit observation probes effectively one scale height of the atmosphere, modulated by the atmospheric opacity at that wavelength. The characteristic transit signal of one scale height is just the ratio of the projected area of the planet's annulus to the area of the host star:

$$\delta = \frac{\delta A}{A} = \frac{2\pi R_P H}{\pi R_*^2}. \tag{787}$$

By observing the transit at multiple wavelengths, one builds up a **transmission spectrum** – the wavelength-dependent transit depth. The difference between the transit depths at two wavelengths is then just

$$\left(\frac{\delta F}{F}\right)_1 - \left(\frac{\delta F}{F}\right)_2 \approx \delta \ln \frac{\sigma_1}{\sigma_2}. \tag{788}$$

In the strongest lines, the core-to-wing opacity ratio might be as high as 10^4, but the logarithmic dependence means that only roughly $10H$ will be probed. Most lines are weaker than this, so in practice transmission spectroscopy probes a moderately narrow range of the atmosphere — frustrating because we can't measure pressures outside of this range, but nice because some of our assumptions (such as that the atmosphere is isothermal) are moderately valid.

One simple, analytic example is Rayleigh scattering, in which $\sigma \propto \lambda^{-4}$ due to small particles (molecules or tiny particulates) high in a planet's atmosphere. In transit, the transit depth will then scale as

$$\delta \ln \frac{\sigma_1}{\sigma_2} \propto (-4 \ln \lambda) \frac{H R_p}{R_*^2}. \quad (789)$$

Equivalently, this means that the apparent planetary radius should increase to shorter wavelengths as

$$R_P(\lambda) \propto -H \ln \lambda \propto \frac{T}{\mu g} \ln \lambda. \quad (790)$$

If transits and radial velocities have measured a planet's R_P, M_p, and so also g, then by measuring the transit spectrum one obtains (in principle) a degenerate measurement of the mean molecular weight μ and the atmospheric temperature T.

In practice, only a few atmospheres obviously show a clear signature of Rayleigh scattering; most have a multitude of opacity sources (often including mid-level-sized clouds or hazes) which complicates the picture. But the general result that transit-inferred planet size is proportional to $\ln \sigma$ remains valid.

26.4 *Basic scaling relations for atmospheric characterization*

There are several fundamental ways that the atmospheres of exoplanets are characterized:

- **Transits.** These measure the planet-to-star radius ratio $\delta = R_P^2/R_*^2$. By inferring the star's properties, we measure the planet size. If we also know its mass, then we know its density and so might know whether it is a puffy gas giant or dense rock. However, the bulk compositions of planets with sizes of 2–6$R_\oplus$ are degenerate – they cannot be uniquely determined by mass and radius measurements alone.

- **Transmission.** As described above, the signal amplitude is roughly HR_P/R_*^2. This is $\propto TR_P/(\mu g_P R_*^2 \propto T/(\mu \rho_P R_*^2)$. So a hot, low-density planet with a H_2-dominated atmosphere will have a large signal – as one moves to cooler and denser planets with heavier atmospheric constituents (i.e., towards more Earth-like planets) characterization becomes progressively more difficult.

- **Thermal Emission: eclipses.** When a transiting planet passes behind its host star, its thermal emission is blocked. To first order, if the planet and star both emit as blackbodies then the measured signal is $\delta(B_\nu(T_P)/B_\nu(T_*))$. If the planets are hot and we observe in the infrared near the Rayleigh-Jeans tail, then (very roughly) we will instead have $\delta T_P/T_*$ – infrared eclipses give us the temperature of the planet. More specifically, this is the brightness temperature of the planet's day side (the only hemisphere seen right around the time of eclipse).

- **Thermal Emission: phase curves.** Most exoplanets are hotter (and brighter) on their daysides and colder (and dimmer) on their nightsides. By observing throughout a planet's orbit, we can sometimes measure the roughly sinusoidal change in system brightness during a full planet orbit. The full (peak-to-valley) amplitude of this flux variation (assuming blackbody emission) will be $\delta(B_\nu(T_{\rm p,hot}) - B_\nu(T_{\rm p,cold}))/B_\nu(T_*))$. In the Rayleigh-Jeans limit, this becomes $\delta(T_{\rm p,hot} - T_{\rm p,cold})/T_*$. With the eclipse observed "for free" during the phase curve, we thus measure the day-to-night temperature contrast. We can actually get a low-resolution 1D (longitudinally-averaged) temperature map of the entire planet.

- **Thermal Emission: direct imaging.** Most known exoplanets are in very short periods and cannot be spatially resolved by telescopes. These observations are dominated by stellar flux and Poisson (photon) noise limits the achievable precision. A few planets are on very wide orbits, such that the stellar light is well-separated from the planet. In these cases one can "simply" point a spectrograph at the planet and measure its emission spectrum, just like one does for a planet. The relative signal amplitude will be the same as for the eclipse case described above, but the relative noise levels will be lower (all else being equal). Like eclipses and phase curves, direct imaging can also in principle be done at visible wavelengths; here the observed planet flux will often be dominated by scattering (and so by the planet's albedo) and not so much by T_P.

The following table gives approximate estimates for the signal amplitude for several different types of planetary systems. It should be apparent why so many more hot Jupiters than habitable, Earthlike planets have been studied: the atmospheric signals for those hot gas giants are orders of magnitude larger.

Method	Scaling	Earth, G2 Dwarf	Hot Jupiter, G2 Dwarf	Earth, M dwarf	Hot Jupiter, M dwarf
$T_{\rm eq}$	$T_{\rm eff}\left(\frac{R_*}{2a}\right)^{1/2}$	280 K	1600 K	280 K	1000 K
Transit	$\left(\frac{R_P}{R_*}\right)^2$	10^{-4}	10^{-2}	6×10^{-4}	6×10^{-2}
Transmission	$\frac{HR_P}{R_*^2}$	10^{-7}	10^{-4}	6×10^{-7}	3×10^{-4}
Emission (5μm)	$\left(\frac{R_P}{R_*}\right)^2\frac{B_\nu(T_P)}{B_\nu(T_*)}$	2×10^{-9}	10^{-3}	2×10^{-8}	6×10^{-3}

26.5 *Thermal Transport: Atmospheric Circulation*

Thermal phase curves in particular offer the intriguing possibility of studying global conditions all around the planet — in contrast to eclipses (which probe only the day-side) and transits (which probe only the day-night terminator). Fully modeling a planet's global atmospheric circulation requires so-called general circulation models (GCMs) that solve some version of the Navier-Stokes fluid equations (and perhaps also accounting for other physics such as ionization, magnetic fields, etc.). Nonetheless we can build a simple thermal transport model to describe what we might expect to see when observing phase curves.

We will consider a day in the life of an individual gas parcel on a tidally-locked, short-period exoplanet. The planet is on a circular orbit and receives incident bolometric flux from its star

$$F_{\rm inc} = \sigma T_{\rm eff}^4 \left(\frac{R_*}{a}\right)^2. \quad (791)$$

However, the gas parcel only absorbs a fraction of this incident flux. This fraction accounts both for the albedo (discussed previously) but also for planetary geometry: planets are spheres, and a gas parcel near the planet's limb or equator will absorb less stellar energy than at noon on the equator (the substellar point). Another way of thinking about this is that solar cells tend to be a lousy investment in Antarctica. Assume the parcel is at latitude θ and longitude ϕ. We define $\theta = 0$ at the North pole and π at the South pole, while $\phi = 0$ at the substellar longitude, $-\pi/2$ at dawn, and $\pi/2$ at sunset.

The net flux of the parcel will be

$$\Delta F = (1 - A_B) F_{\rm inc} \sin\theta \max(\cos\phi, 0) - \sigma T^4. \quad (792)$$

(The "max" function takes the maximum of the two arguments, and accounts for the fact that when our atmosphereic parcel is on the night side, it absorbs zero (not negative) flux.) If the parcel has density ρ, specific heat capacity c_P, and thickness H then we obtain a differential equation for the parcel's temperature:

$$\frac{dT}{dt} = \frac{1}{c_h}\left((1 - A_B) F \sin\theta \max(\cos\phi, 0) - \sigma T^4\right) \quad (793)$$

where

$$c_h = \rho c_P H. \quad (794)$$

If we set $dT/dt = 0$ in Eq. 793, then we obtain an expression for the *local* equilibrium temperature of the gas parcel.

Since one parcel is as good as another, if we can solve Eq. 793 for one gas parcel and relate time to the parcel's longitude then we will know how the surface temperature of the entire planet varies with longitude – i.e., we will have constructed a planetary temperature map.

To make things a bit more tractable, we define a fiducial temperature

$$T_0 \equiv T_{\rm eff}(1-A_B)^{1/4}\sin^{1/4}\theta\left(\frac{R_*}{a}\right)^{1/2} \quad (795)$$

and also define the **radiative timescale**

$$\tau_{\rm rad} \equiv \frac{c_h}{\sigma T_0^3}. \quad (796)$$

If we then define a dimensionless temperature $T' \equiv T/T_0$ and time $t' \equiv t/\tau_{\rm rad}$, then Eq. 793 is simplified to

$$\frac{dT'}{dt'} = \max(\cos\phi, 0) - T'^4. \quad (797)$$

This is a function of time, but we could also write things in terms of longitude if we could describe the motion of our gas parcel around the planet. We assume that our gas parcel is advected around the planet (e.g., by the globally circulating winds predicted on hot gas giants) with a characteristic windspeed $v_{\rm adv}$, giving rise to a characteristic **advective timescale**

$$\tau_{\rm adv} \equiv \frac{2\pi R_P}{v_{\rm adv}}. \quad (798)$$

An important quantity is the ratio of these two timescales, which we denote

$$\epsilon \equiv \frac{\tau_{\rm rad}}{\tau_{\rm adv}}. \quad (799)$$

When $\epsilon \ll 1$, radiation is "faster" (i.e., more efficient) than advection and energy is almost immediately radiated away before it can be transported around the planet. When $\epsilon \gg 1$, the reverse is true and energy is swept away by winds much more rapidly than it can be re-radiated. Eq. 797 then becomes

$$\frac{dT'}{d\phi} = \frac{2\pi}{\epsilon}\left(\max(\cos\phi, 0) - T'^4\right). \quad (800)$$

Eq. 800 has two solutions, depending on whether the parcel is on the day side (absorbing energy while re-radiating) or on the night side (emitting only). The analytic solution for the night-side temperature can be found by integrating from dusk (when the parcel stops absorbing energy, $\phi = \pi/2$) until some later phase ϕ (up until dawn). The solution is

$$T'_{\rm night}(\phi) = \left(\frac{6\pi}{\epsilon}\left[\phi - \frac{\pi}{2}\right] + (T'_{\rm dusk})^{-3}\right)^{-1/3}. \quad (801)$$

If advection is extremely efficient, then the first term in parentheses is zero and $T_{\rm night} = T_{\rm dusk}$ — the planet's night side has a uniform temperature. But as radiative transport begins to dominate advective heat transport, the night side

temperature will drop steadily from dusk (consisting of parcels that only just stopped seeing their star) to dawn (after they have been radiating away thermal energy for the entire night). Note that this process happens even though the planet itself is tidally locked; global winds still circulate.

On the day side, there is no general analytic solution to Eq. 800 (though it can be solved numerically). Nonetheless (as with the night side) the solution will depend sensitively on the ratio of advective and radiative timescales. If $\epsilon \gg 1$ then advection is very efficient, and

$$\frac{dT'_{\rm day}}{d\phi} = 0 \;\rightarrow\; T_{\rm day} = \text{const.} \tag{802}$$

If energy transport is very efficient, the temperature is the same, day and night. On the other hand, if $\epsilon \ll 1$ then radiation is extremely efficient and winds have negligible effect on heat transport. In that case,

$$T'_{\rm day} = \cos^{1/4}\phi. \tag{803}$$

As the next-order approximation, one can assume that T' is a quadratic

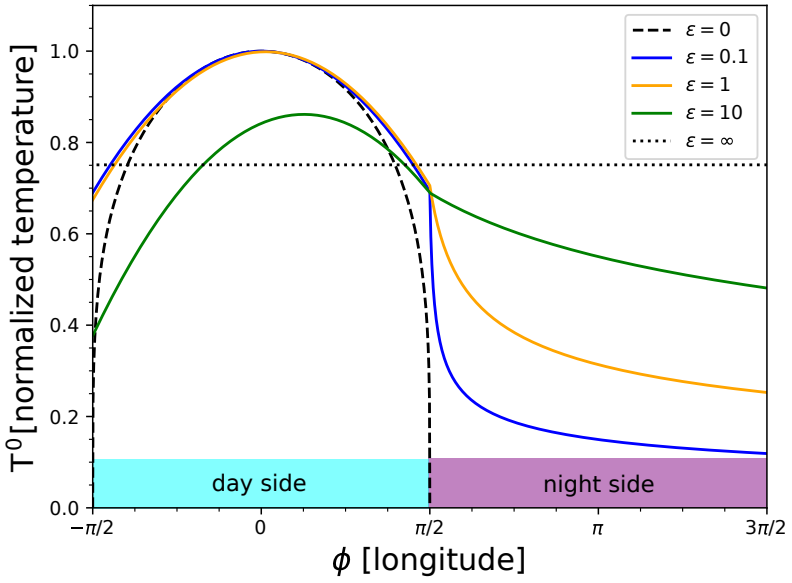

Figure 64: Planetary temperature vs. longitude for a simple energy transport model, for different values of $\epsilon = \tau_{\rm rad}/\tau_{\rm adv}$. The substellar longitude is at $\phi = 0$. The solid curves on the day side are the second-order approximate solutions of Eq. 804, while on the night side are plotted the exact solutions of Eq. 801. The broken black curves are the exact solutions for the limiting cases indicated, i.e. atmospheres dominated by radiation (dashed) and advection (dotted).

function of ϕ and similarly expand $\cos\phi$ to second order. This is a pretty crude model, but it provides one or two final insights. Under this assumption, setting $\epsilon \equiv \tau_{\rm rad}/\tau_{\rm adv}$ yields

$$T_{\rm day} \approx \left(1 - \frac{\epsilon^2}{64\pi^2}\right) + \frac{\epsilon}{32\pi}\phi - \frac{1}{8}\phi^2. \tag{804}$$

These approximate solutions are plotted in Fig. 64 for several values of ϵ. Note that the low-ϵ curves are a decent match to the exact analytic solution for $\epsilon = 0$ (i.e., Eq. 803), but the quadratic models overpredict the temperature at dawn and dusk. They also leave a discontinuity in T' at dawn; this can be fixed by computing the full numerical solution to Eq. 800.

The temperature of our circulating gas parcel reaches a maximum when $dT'/d\phi = 0$, which implies a longitude of maximum temperature

$$\phi_{\rm max} \approx \frac{1}{8\pi}\frac{\tau_{\rm rad}}{\tau_{\rm adv}}. \tag{805}$$

Thus the hottest part of the planet is located to the East of the substellar point; this shift in peak temperature is the **phase offset**, and gives an estimate of the relative timescales operating in a planet's atmosphere. (This is *not* the reason that on Earth it's warmer in the early afternoon than at dead noon; that's because of the Earth's thermal intertia and its rapid rotation, $P_{\rm rot}/P_{\rm orb} \ll 1$.)

By setting $\phi = \phi_{\rm max}$ in Eq. 804, we obtain the maximum dayside temperature:

$$T'_{\rm day,max} = T'_{\rm day}(\phi_{\rm max}) \approx 1 - \frac{7\epsilon^2}{512\pi^2}. \tag{806}$$

Thus radiative-dominated atmospheres have the maximum possible day side temperatures. As advection plays an increasingly important role, more energy is distributed around the planet and the maximum day side temperature decreases. In the exact solution, the maximum temperature also correlates with the phase offset, as

$$T'_{\rm max} = \cos^{1/4}\phi_{\rm max} \tag{807}$$

down to a minimum of $\pi^{-1/4}$ (as plotted in Fig. 64).

Many typical hot Jupiters have phase offsets of $\sim 20^o$ — indicating typical values of $\epsilon \approx 10$, day side temperatures 10–15% cooler than in local equilibrium, and moderate day-to-night temperature contrasts. As one observes hotter and hotter planets (e.g., $T_{\rm eq} \gtrsim 2000$ K), radiation increasingly dominates over heat transport, $\epsilon \to 0$, day sides become hotter, and day-night temperature contrast increases. In practice, processes other than radiation and advection become important when considering atmospheric circulation; in particular, various drag forces and their associated timescales can become at least as relevant as the advective processes that they inhibit.